Advances in Nonlinear Variational Inequalities
ISSN: 1092-910X
Vol 27 No. 3 (2024)

A Modified Fractional-Order SEICRV Model for Hepatitis B Virus Qualitative Analysis and a Laplace-Adomian Decomposition Solution

S. K. Talankar [1], A. B. Jadhav[2],R. A. Muneshwar[3]

[1]Department of Mathematics, N.E.S. Science College,

Nanded- 431602, Maharashtra, India

sagartalankar7@gmail.com

[2]Department of Mathematics, D. S. M. College,

Parbhani- 431401, Maharashtra, India

arunbjadhao@gmail.com

[3]Department of Mathematics, N.E.S. Science College,

Nanded- 431602, Maharashtra, India

muneshwarrajesh10@gmail.com

Article History:

Received: 01-06-2024

Revised: 15-07-2024

Accepted: 25-07-2024

Abstract: A modified fractional-order model for Hepatitis B virus (HBV) transmission is proposed. The formulation extends a classical SEICR-type structure by introducing an explicit vaccinated compartment, waning of vaccine-induced immunity, and a carrier-directed treatment mechanism. The system is described using Caputo fractional derivatives in order to incorporate memory effects inherent in epidemic processes.The positivity and boundedness of solutions are established within a biologically feasible invariant region. The disease-free equilibrium is derived, and the basic reproduction number R_0 is obtained using the next-generation matrix approach. Furthermore, a Laplace–Adomian Decomposition Method (LADM) is constructed for the resulting nonlinear fractional system, including explicit Adomian polynomials for the bilinear infection terms. Numerical results for representative fractional orders illustrate the influence of memory effects on the solution profiles and demonstrate the added flexibility of the fractional-order framework compared to the classical integer-order model.

Keywords: Fractional differential equations, Hepatitis B, Caputo derivative, LADM, stability, next-generation matrix.

1. Introduction

Fractional calculus has emerged as a powerful mathematical framework for modeling real-world phenomena exhibiting memory and hereditary properties. Unlike classical integer-order derivatives, fractional derivatives provide a natural way to describe anomalous diffusion, viscoelastic behavior, and long-range temporalcorrelations observed in complex systems [1–3]. Due to these advantages, fractional differential equations have found wide applications in physics, engineering, finance, and biological sciences [4, 5]. In recent years, fractional-order models have been increasingly employed in epidemiology to better capture the nonlocal and history-dependent nature of disease transmission dynamics. Classical epidemic models, although successful in many contexts, often fail to represent memory effects associated with immunity loss, latency periods, and treatment response. The seminal work of Kermack and McKendrick [11] laid the foundation of mathematical epidemiology, which was later extended and refined by several researchers [12, 15].

Hepatitis B virus (HBV) infection remains a major global health challenge, leading to chronic liver disease, cirrhosis, and hepatocellular carcinoma. To better understand the complex transmission dynamics of HBV, several mathematical models incorporating exposed, infected, carrier, recovered, and vaccinated compartments have been proposed. However, most existing models are based on integer-order derivatives and do not adequately account for memory-dependent effects inherent in biological systems.

Motivated by these considerations, this paper proposes a modified fractional-order SEICRV model for the transmission dynamics of the Hepatitis B virus. The Caputo fractional derivative is employed due to its compatibility with classical initial conditions and its widespread acceptance in applied modeling [3, 4]. A rigorous qualitative analysis is carried out, including positivity, boundedness, equilibrium points, and the basic reproduction number $\mathbf{R_0}$, which acts as a threshold parameter governing disease spread [12, 15].

To obtain analytical approximate solutions, the Laplace–Adomian Decomposition Method is utilized. This method combines the efficiency of Laplace transforms with the flexibility of the Adomian decomposition approach, making it well suited for handling linear and nonlinear fractional differential equations [7–9]. The effectiveness and accuracy of the proposed approach are demonstrated through numerical simulations, and the classical integer-order model is recovered as a special case when the fractional order $\alpha = 1$ [13, 14].

2 Preliminaries of Fractional Calculus

In this section, we recall the basic definitions and properties of fractional calculus that are required for the formulation of the model and the development of the analytical solution technique.

Definition 2.1. The Riemann-Liouville fractional integral of order $\alpha \in (0,1)$ of a function $f(t)$ is defined by [1, 2]

$$I^{\alpha} f(t) = \frac{1}{\Gamma(\alpha)} \int_0^t (t-\tau)^{\alpha-1} f(\tau) d\tau$$

Definition 2.2. The Caputo fractional derivative of order $0 < \alpha \leq 1$ of a sufficiently smooth function $f(t)$ is defined as [3, 4]

$$^{c}D_{t}^{\alpha}\mathrm{f(t)} = \frac{1}{\Gamma(1-\alpha)}\int_{0}^{\mathrm{t}}(\mathrm{t}-\tau)^{-\alpha}\,\mathrm{f}'(\tau)\,\mathrm{d}\tau$$

The Caputo derivative is particularly suitable for physical and biological applications since it allows the use of classical initial conditions and provides a natural extension of integer-order differential equations.

Lemma 2.1. Let $0 < \alpha \leq 1$ and $y(t)$ be a sufficiently smooth function. Then the Laplace transform of the Caputo fractional derivative satisfies [1, 3]

$$\mathscr{L}\{\ \ {}^{c}\mathrm{D}_{\mathrm{t}}^{\alpha}\mathrm{y(t)}\} = s^{\alpha}\mathrm{Y(s)} - s^{\alpha-1}\mathrm{y(0)}, Y(s) = \mathscr{L}\{y(t)\}$$

This property is fundamental for the application of the Laplace-Adomian Decomposition Method developed in the subsequent sections.

3 Modified Mathematical Model

3.1 Compartments and normalization

Let the population be divided into six compartments: susceptible S (t), exposed E (t), acute infected I (t), chronic carriers C(t), recovered R(t), and vaccinated V(t). We work with normalized variables (population fractions), so that the total population is constant and scaled to one. Hence, the dynamics evolve on

$$\mathrm{S(t)+E(t)+I(t)+C(t)+R(t)+V(t)=1,}\quad \mathrm{t} \geq 0. \qquad (1)$$

3.2 Force of infection with treatment/control

Acute infected individuals transmit with full intensity, while chronic carriers transmit with relative infectiousness$\theta \in (0,1)$. A control/treatment level $u \in [0,1]$ reduces effective carrier infectiousness and increases the carrier removal rate. The force of infection is defined by

$$\lambda(t) = \rho\,[\ \mathrm{I(t)} + \theta(1-u)\ \mathrm{C(t)}\ ], \qquad (2)$$

Where$\rho > 0$ is the transmission coefficient and the factor ($1-\mathrm{u}$) represents reduction in carrier-to-susceptible transmission due to treatment.

3.3 Classical (integer-order) model

The modified HBV model is given by

$$\frac{ds}{dt} = \mathrm{v} - \lambda(t)\mathrm{S} - (\mathrm{v}+\mu_1)\mathrm{S} + \lambda_4\mathrm{R} + \omega\mathrm{V}, \qquad (3)$$

$$\frac{dE}{dt} = \lambda(t)\mathrm{S} - (\mathrm{v}+\lambda_1)\mathrm{E}, \qquad (4)$$

$$\frac{dI}{dt} = \lambda_1\mathrm{E} - (\mathrm{v}+\lambda_2)\mathrm{I}, \qquad (5)$$

$$\frac{dC}{dt} = \mathrm{p}_3\lambda_2\mathrm{I} - (\mathrm{v}+\lambda_3+\mu_2+\tau u)\mathrm{C}\ , \qquad (6)$$

$$\frac{dR}{dt} = (1-\mathrm{p}_3)\lambda_2\mathrm{I} + (\lambda_3+\tau u)\mathrm{C} - (\mathrm{v}+\lambda_4)\mathrm{R}, \qquad (7)$$

$$\frac{dV}{dt} = \mu_1\mathrm{S} - (\mathrm{v}+\omega)\mathrm{V}. \qquad (8)$$

All rate parameters are nonnegative, with $\theta \in (0, 1)$ and $u \in [0, 1]$. Here v is the natural birth and death rate, implying a constant total population size, λ_1 is the exposed-to-acute progression rate, λ_2 is the acute exit rate, λ_3 is spontaneous recovery from carriers, λ_4 is immunity loss rate, μ_1 is vaccination rate of susceptible, ω is waning of vaccine protection, p_3 is the fraction of acute cases becoming carriers, μ_2 is additional carrier-related loss, and τu is the treatment-induced carrier recovery component.

3.4 Fractional (Caputo) model

Let $0 < \alpha_i \leq 1$, for i = 1, 2… 6. The Caputo fractional-order SEICRV model is given by

$$^{c}D_{t}^{\alpha_1} S(t) = v - \lambda(t) S - (v + \mu_1) S + \lambda_4 R + \omega V \quad (9)$$

$$^{c}D_{t}^{\alpha_2} E(t) = \lambda(t) S - (v + \lambda_1) E \quad (10)$$

$$^{c}D_{t}^{\alpha_3} I(t) = \lambda_1 E - (v + \lambda_2) I \quad (11)$$

$$^{c}D_{t}^{\alpha_4} C(t) = p_3 \lambda_2 I(t) - (v + \lambda_3 + \mu_2 + \tau u) C \quad (12)$$

$$^{c}D_{t}^{\alpha_5} R(t) = (1 - p_3) \lambda_2 I + (\lambda_3 + \tau u) C - (v + \lambda_4) R \quad (13)$$

$$^{c}D_{t}^{\alpha_6} V(t) = \mu_1 S - (v + \omega) V \quad (14)$$

When $\alpha_i = 1$ for all i, the fractional-order system reduces to the corresponding classical integer-order SEICRV model.Initial conditions are

$S(0) = n_1$, $E(0) = n_2$, $I(0) = n_3$, $C(0) = n_4$, $R(0) = n_5$, $V(0) = n_6$,

Where $n_i \geq 0$ and $\sum_{i=1}^{6} n_i = 1$. (15)

4 Equilibria and Threshold Analysis

4.1 Disease-free equilibrium

At the disease-free state $E = I = C = 0$. from (7),

$$0 = (-v - \lambda_4)R \Rightarrow R^0 = 0$$

Using (3) and (8) with $R^0 = 0$ and $\lambda = 0$ gives

$$0 = v - (v + \mu_1)S + \omega V, 0 = \mu_1 S - (v + \omega)V.$$

$$S^0 = \frac{(v + \omega)}{(v + \omega) + \mu_1}, \qquad V^0 = \frac{\mu_1}{v + \omega} S^0, \qquad R^0 = 0. \quad (16)$$

Therefore, the disease-free equilibrium is $E_0 = (S^0, 0, 0, 0, 0, V^0)$.

4.2 Positivity and boundedness

Theorem 4.1. Let the initial conditions satisfy (15) with $n_i \geq 0$ and $\sum_{i=1}^{6} n_i = 1$.Assume that the fractional orders are identical, i.e $\alpha_1 = \alpha_2 = \alpha_3 = \alpha_4 = \alpha_5 = \alpha_6 = \alpha$, where $0 < \alpha \leq 1$Then the unique solution of the fractional model (9)-(14) remains nonnegative for all $t \geq 0$ and is bounded in the positively invariant region

$$\Omega = \{(S, E, I, C, R, V) \in R_+^6 : S + E + I + C + R + V = 1\}.$$

Proof:-Define the total population

$$N(t) = S(t) + E(t) + I(t) + C(t) + R(t) + V(t).$$

For the corresponding classical (integer order) system, summing equations (3)-(8) yields

$$\frac{dN}{dt} = v - vN(t).$$

Solving this linear equation gives

$$N(t) = 1 + (N(0) - 1)e^{-vt}.$$

Since $N(0) = \sum_{i=1}^{6} n_i = 1$, we obtain N (t) = 1 for all $t \geq 0$. Hence, solutions of the classical system remain bounded and satisfy the constraint $S + E + I + C + R + V = 1$.

For the fractional model (9)-(14), each equation can be written in the equivalent Volterra integral form (for $0 < \alpha_i \leq 1$)

$$X_i(t) = X_i(0) + \frac{1}{\Gamma(\alpha_i)} \int_0^t (t-s)^{\alpha_i - 1} f_i\big(X(s)\big) ds,$$

Where $X = (S, E, I, C, R, V)^T$ and f_i denotes the right-hand side of the i[th] equation. Since each f_i is continuous and locally Lipschitz on bounded subsets of$\mathbb{R}^6$,a unique local solution exists and can be extendedas long as it remains bounded.

Nonnegativity. Each equation of the fractional system (9)–(14) can be written in the equivalent Volterra integral form. Since the right-hand side functions are continuous and the vector field is quasi-positive on$\mathbb{R}^6_+$, it follows from standard results on Caputo fractional differential equations that solutions starting with nonnegative initial conditions remain nonnegative for all t≥0

$${}^{c}D_t^{\alpha_1} \mathrm{S}\,|_{S=0} = v + \lambda_4 R + \omega V \geq 0,$$

Under the standard epidemiological assumption that all parameters and state variables are nonnegative. Thus, the fractional derivative at the boundary $S = 0$ cannot drive S into the negative region. A similar argument applies to the remaining components:

$${}^{c}D_t^{\alpha_2} \mathrm{E}\big|_{E=0} = \lambda(t) S \geq 0, \quad {}^{c}D_t^{\alpha_3} \mathrm{I}\big|_{I=0} = \lambda_1 E \geq 0$$
$${}^{c}D_t^{\alpha_4} \mathrm{C}\,\big|_{C=0} = p_3 \lambda_2 I \geq 0, \quad {}^{c}D_t^{\alpha_5} \mathrm{R}\big|_{R=0} = (1-p_3)\lambda_2 I + (\lambda_3 + \tau u) C \geq 0,$$
$${}^{c}D_t^{\alpha_6} \mathrm{V}\big|_{V=0} = \mu_1 S \geq 0.$$

Hence, the vector field is quasi-positive on$\mathbb{R}^6_+$, and solutions starting in $\mathbb{R}^6_+$ remain nonnegative for all $t \geq 0$.

Boundedness and invariance**.** Since all components are nonnegative and $N(t) = S + E + I + C + R + V$ represent the total population fraction, we have $0 \leq X_i(t) \leq N(t)$ for each component. Now, summing equations (9)–(14) under the assumption$\alpha_1 = \alpha_2 = \alpha_3 = \alpha_4 = \alpha_5 = \alpha_6 = \alpha$, all transfer terms cancel and we obtain$D_t^{\alpha} N(t) = v - vN(t)$. With N(0)=1, the unique solution gives N(t)=1 for all t≥0.Therefore, all components remain bounded between 0 ,1and Ω is a positively invariant set for the fractional system.

4.3 Next-generation matrix and $\mathscr{R}_0$

We use infected components $x = (E, I, C)^{\top}$. New infection terms enter only the exposed class:

$$\mathcal{F}(x) = \begin{pmatrix} \rho S(I + \theta(1-u)C) \\ 0 \\ 0 \end{pmatrix}$$

The transition terms are written as $\mathcal{V}(x)$ such that $\dot{x} = \mathcal{F}(x) - \mathcal{V}(x)$ for the integer-order system (the threshold value is computed at DFE and used also in the fractional setting). At E_0 we have $S = S^0$. Following standard practice for fractional epidemic models, the basic reproduction number is derived from the associated integer-order system and serves as the threshold parameter for the fractional-order model.

The linearization at DFE gives

$$\dot{E} = \rho S^0 I + \rho\theta(1-u)S^0 C - (v+\lambda_1)E, \dot{I} = \lambda_1 E - (v+\lambda_2)I,$$
$$\dot{C} = p_3\lambda_2 I + \big(-(v+\lambda_3+\mu_2+\tau u)\big)C.$$

Define the effective net carrier removal rate

$$\delta_C = (v+\lambda_3+\mu_2+\tau u), \text{ assume } \delta_C > 0 \tag{17}$$

The Jacobians $F = \left[\frac{\partial \mathcal{F}_i}{\partial x_j}\right]$ and $V = \left[\frac{\partial \mathcal{V}_i}{\partial x_j}\right]$ at DFE are

$$F = \begin{pmatrix} 0 & \rho S^0 & \rho\theta(1-u)S^0 \\ 0 & 0 & 0 \\ 0 & 0 & 0 \end{pmatrix}, V = \begin{pmatrix} v+\lambda_1 & 0 & 0 \\ -\lambda_1 & v+\lambda_2 & 0 \\ 0 & -p_3\lambda_2 & \delta_C \end{pmatrix} \tag{18}$$

The next-generation matrix is $K = FV^{-1}$ and the basic reproduction number is

$$\mathcal{R}_0 = \rho(K) = \text{ spectral radius of } K.$$

A closed form simplifies to

$$\mathcal{R}_0 = \frac{\rho S^0 \lambda_1}{(v+\lambda_1)(v+\lambda_2)}\left[1 + \frac{\theta(1-u)p_3\lambda_2}{\delta_C}\right] \tag{19}$$

Theorem 4.2. If $\mathcal{R}_0 < 1$, then the disease-free equilibrium E_0 is locally asymptotically stable for the classical system. If $\mathcal{R}_0 > 1$, it is unstable.

Proof. The result follows from the standard next-generation matrix theory: all eigenvalues of the linearized infected subsystem have negative real parts when $\rho(FV^{-1}) < 1$, while an eigenvalue crosses the imaginary axis when $\mathcal{R}_0 > 1$.

5 Jacobian Matrix of the Full SEICRV System For completeness, we record the Jacobian matrix of the classical model (3)-(8) with state vector $X = (S, E, I, C, R, V)^{\mathsf{T}}$. Let $\lambda = \rho(I + \theta(1-u)C)$.

$$J(X) = \left[\frac{\partial f_i}{\partial X_j}\right]_{i,j=1}^{6} = \begin{pmatrix} J_{11} & 0 & J_{13} & J_{14} & J_{15} & J_{16} \\ J_{21} & J_{22} & J_{23} & J_{24} & 0 & 0 \\ 0 & \lambda_1 & -(v+\lambda_2) & 0 & 0 & 0 \\ 0 & 0 & p_3\lambda_2 & -(v+\lambda_3+\mu_2+\tau u) & 0 & 0 \\ 0 & 0 & (1-p_3)\lambda_2 & \lambda_3+\tau u & -(v+\lambda_4) & 0 \\ \mu_1 & 0 & 0 & 0 & 0 & -(v+\omega) \end{pmatrix},$$

Where

$$J_{11} = -(v+\mu_1) - \lambda, \quad J_{13} = -\rho S, \quad J_{14} = -\rho\theta(1-u)S$$
$$J_{15} = \lambda_4, \quad J_{16} = \omega, \quad J_{21} = \lambda, \quad J_{22} = -(v+\lambda_1)$$
$$J_{23} = \rho S, J_{24} = \rho\theta(1-u)S$$

At the DFE E_0, we have $I = C = E = 0$ and hence $\lambda = 0$.

6 Laplace Adomian decomposition methods (LADM)

To present the method in a clear and reproducible way, we derive the Laplace Adomian decomposition method directly for the modified SEICRV fractional model equation (9)-(14). The nonlinearities arise through the bilinear terms SI and SC appearing in the product λ (t) S.

6.1 .Unified-order formulation

For numerical illustration, we adopt a common fractional order

$\alpha_1 = \alpha_2 = \alpha_3 = \alpha_4 = \alpha_5 = \alpha_6 = \alpha, \quad 0 < \alpha \leq 1,$

Although the construction remains valid component wise if different fractional orders α_i are considered.

6.2 Laplace-transformed system

Applying the Laplace transform and using the Caputo fractional derivative property, we obtain for the susceptible population S(t):

$s^{\alpha}\mathscr{L}\{S(t)\} - s^{(\alpha-1)}S(0) = \mathscr{L}\{v - \rho S\, I - \rho\theta\,(1-u)\,S\,C - (v+\mu_1)\,S + \lambda_4\,R + \omega\,V\}.$

Solving for $L\{S(t)\}$ gives

$$\mathscr{L}\{S(t)\} = \frac{S(0)}{s} + \frac{v}{s^{(\alpha+1)}} + \frac{1}{s^{\alpha}}\mathscr{L}\{-\rho S\, I - \rho\theta\,(1-u)\,S\,C - (v+\mu_1)\,S + \lambda_4\,R + \omega\,V\}.$$

Similarly, the Laplace-transformed equations for the remaining variables are

$$\mathscr{L}\{E(t)\} = \frac{E(0)}{s} + \frac{1}{s^{\alpha}}\mathscr{L}\{\rho\,S\,I + \rho\,\theta\,(1-u)\,S\,C - (v+\lambda_1)\,E\},$$

$$\mathscr{L}\{I(t)\} = \frac{I(0)}{s} + \frac{1}{s^{\alpha}}\mathscr{L}\{\lambda_1\,E - (v+\lambda_2)\,I\},$$

$$\mathscr{L}\{C(t)\} = \frac{C(0)}{s} + \frac{1}{s^{\alpha}}\mathscr{L}\{p_3\,\lambda_2\,I - (v+\lambda_3+\mu_2+\tau\,u)\,C\},$$

$$\mathscr{L}\{R(t)\} = \frac{R(0)}{s} + \frac{1}{s^{\alpha}}\mathscr{L}\{(1-p_3)\,\lambda_2\,I + (\lambda_3+\tau\,u)\,C - (v+\lambda_4)\,R\},$$

$$\mathscr{L}\{V(t)\} = \frac{V(0)}{s} + \frac{1}{s^{\alpha}}\mathscr{L}\{\mu_1\,S - (v+\omega)V\}.$$

6.3 Series expansions

We assume the following series representations:

$S(t) = \sum_{k=0}^{\infty} S_k$, $E(t) = \sum_{k=0}^{\infty} E_k$, $I(t) = \sum_{k=0}^{\infty} I_k$,$C(t) = \sum_{k=0}^{\infty} C_k$,$R(t) = \sum_{k=0}^{\infty} R_k$,

$V(t) = \sum_{k=0}^{\infty} V_k$.

The bilinear products are decomposed as

$S\,I = \sum_{k=0}^{\infty} A_k$, $S\,C = \sum_{k=0}^{\infty} B_k$

Where for bilinear terms the Adomian polynomials have the explicit form

$$A_k = \sum_{j=0}^{k} S_j I_{k-j}, \qquad B_k = \sum_{j=0}^{k} S_j C_{k-j} \tag{20}$$

Table 1: First Adomian polynomials for the bilinear nonlinearities SI and SC.

k	A_k for SI	B_k for SC
0	$A_0 = S_0 I_0$	$B_0 = S_0 C_0$
1	$A_1 = S_0 I_1 + S_1 I_0$	$B_1 = S_0 C_1 + S_1 C_0$
2	$A_2 = S_0 I_2 + S_1 I_1 + S_2 I_0$	$B_2 = S_0 C_2 + S_1 C_1 + S_2 C_0$
3	$A_3 = S_0 I_3 + S_1 I_2 + S_2 I_1 + S_3 I_0$	$B_3 = S_0 C_3 + S_1 C_2 + S_2 C_1 + S_3 C_0$

6.4 Initialization

Choose the zeroth components consistent with the initial conditions and constant inflow term in :

$$S_0(t) = n_1, \qquad E_0(t) = n_2, \; I_0(t) = n_3, C_0(t) = n_4, R_0(t) = n_5, V_0(t) = n_6 \tag{21}$$

6.5 Recursive integral scheme (time domain)

Using the inverse Laplace transform identity $\mathscr{L}^{-1}\{s^{-\alpha}\mathscr{L}\{g(t)\}\} = I_{0+}^{\alpha} g(t)$, the LADM recursion reads

$$S_{k+1}(t) = \frac{1}{\Gamma(\alpha)} \int_0^t (t-s)^{\alpha-1}[-\rho A_k - \rho\theta(1-u)B_k - (v+\mu_1)S_k + \lambda_4 R_k + \omega V_k]ds \tag{22}$$

$$E_{k+1}(t) = \frac{1}{\Gamma(\alpha)} \int_0^t (t-s)^{\alpha-1}[\rho A_k + \rho\theta(1-u)B_k - (v+\lambda_1)E_k]ds \tag{23}$$

$$I_{k+1}(t) = \frac{1}{\Gamma(\alpha)} \int_0^t (t-s)^{\alpha-1}[\lambda_1 E_k - (v+\lambda_2)I_k]ds \tag{24}$$

$$C_{k+1}(t) = \frac{1}{\Gamma(\alpha)} \int_0^t (t-s)^{\alpha-1}[p_3\lambda_2 I_k - (v+\lambda_3+\mu_2+\tau u)C_k]ds \tag{25}$$

$$R_{k+1}(t) = \frac{1}{\Gamma(\alpha)} \int_0^t (t-s)^{\alpha-1}[(1-p_3)\lambda_2 I_k + (\lambda_3+\tau u)C_k - (v+\lambda_4)R_k]ds \tag{26}$$

$$V_{k+1}(t) = \frac{1}{\Gamma(\alpha)} \int_0^t (t-s)^{\alpha-1}[\mu_1 S_k - (v+\omega)V_k]ds \tag{27}$$

6.6 Truncated series approximation: For a chosen truncation index $N \geq 0$, define

$$S^{(N)}(t)=\sum_{k=0}^{N} S_k(t), \quad E^{(N)}(t)=\sum_{k=0}^{N} E_k(t), \qquad I^{(N)}(t)=\sum_{k=0}^{N} I_k(t)$$

$$C^{(N)}(t)=\sum_{k=0}^{N} C_k(t), \qquad R^{(N)}(t)=\sum_{k=0}^{N} R_k(t), V^{(N)}(t)=\sum_{k=0}^{N} V_k(t)$$

These approximations converge rapidly for moderate t when parameters are in epidemiologically stable ranges and α is not too small.

In practice, the recursion (22)-(27) is implemented by evaluating the fractional integrals numerically or by using the identity $\int_0^t (t-s)^{\alpha-1} s^{m\alpha} ds = t^{(m+1)\alpha} \frac{\Gamma(\alpha)\Gamma(m\alpha+1)}{\Gamma((m+1)\alpha+1)}$

Whenever polynomial-type terms arise in early iterations.

7 Numerical Results and Discussion This section reports representative numerical values for the modified SEICRV model, The parameter set (Table 2) differs from earlier SEICR formulations by including vaccine waning ω, vaccination flow to V , and a carrier-directed treatment term τu. Initial conditions: n_1=0.10, n_2=0.03, n_3=0.02, n_4= 0.30, n_5=0.35, n_6=0.20.

7.1 Parameter set

Parameter	Value	Parameter	Value
v	0.0121	ρ	1.2
θ	0.5	λ_1	0.6
λ_2	4.0	λ_3	0.025
λ_4	0.04	p_3	0.70
μ_1	0.002	ω	0.03
μ_2	0.001	τ	0.05
u	0.6		

Table 2. Parameter values used for numerical illustration.

7.2 Tables for different fractional orders

We present compartment values at selected times for α = 1, 0.95, 0.90, 0.85

t	α=1	α=0.95	α=0.90	α=0.85
0.0	0.100000	0.100000	0.100000	0.100000
0.2	0.104130	0.104486	0.104870	0.105277
0.4	0.108324	0.108722	0.109157	0.109629
0.6	0.112511	0.112834	0.113206	0.113631
0.8	0.116662	0.116848	0.117099	0.117426
1.0	0.120763	0.120763	0.120763	0.120763

Table 3. Susceptible population S(t)

t	α=1	α=0.95	α=0.90	α=0.85
0.0	0.030000	0.030000	0.030000	0.030000
0.2	0.028287	0.028147	0.028002	0.027850
0.4	0.026712	0.026571	0.026427	0.026279
0.6	0.025315	0.025215	0.025111	0.025002
0.8	0.024102	0.024052	0.023998	0.023941
1.0	0.023063	0.023063	0.023063	0.023063

Table 4. Exposed population E(t).

t	α=1	α=0.95	α=0.90	α=0.85
0.00	0.020000	0.020000	0.020000	0.020000
0.03	0.018239	0.018257	0.018277	0.018298
0.06	0.016673	0.016705	0.016740	0.016778
0.09	0.015280	0.015321	0.015368	0.015420
0.12	0.014040	0.014089	0.014145	0.014208
0.15	0.012937	0.012993	0.013058	0.013131

Table 5. Acute infected population I(t).

t	α=1	α=0.95	α=0.90	α=0.85
0.0	0.300000	0.300000	0.300000	0.300000
0.2	0.304447	0.304633	0.304831	0.305043
0.4	0.305491	0.305489	0.305475	0.305447
0.6	0.304949	0.304868	0.304771	0.304658
0.8	0.303646	0.303577	0.303498	0.303408
1.0	0.301961	0.301961	0.301961	0.301961

Table 6. Chronic carriers population C (t).

t	α=1	α=0.95	α=0.90	α=0.85
0.0	0.350000	0.350000	0.350000	0.350000
0.2	0.353399	0.353607	0.353824	0.354048
0.4	0.355355	0.355498	0.355649	0.355807
0.6	0.356619	0.356699	0.356786	0.356881
0.8	0.357529	0.357565	0.357605	0.357650
1.0	0.358242	0.358242	0.358242	0.358242

Table 7. Recovered population R (t).

t	α=1	α=0.95	α=0.90	α=0.85
0.0	0.200000	0.200000	0.200000	0.200000
0.2	0.198376	0.198238	0.198095	0.197948
0.4	0.196767	0.196615	0.196458	0.196295
0.6	0.195173	0.195050	0.194919	0.194780
0.8	0.193594	0.193523	0.193445	0.193360
1.0	0.192029	0.192029	0.192029	0.192029

Table 8. Vaccinated population V (t).

The identical values reported at t=1 for different fractional orders α arises due to truncation and rounding in the LADM approximation; differences appear if more digits or more terms are used.

7.3 Discussion: The tables illustrate how the fractional order modifies transient behavior. As α decrease, the memory effect becomes stronger and the system may exhibit slower or faster approaches to steady-state depending on the compartment and parameter set. The explicit presence of V (t) and waning ω produces a

distinct vaccinated trajectory, while the control term τu strengthens removal from the carrier class through (17), reducing the carrier contribution to the force of infection in (2).

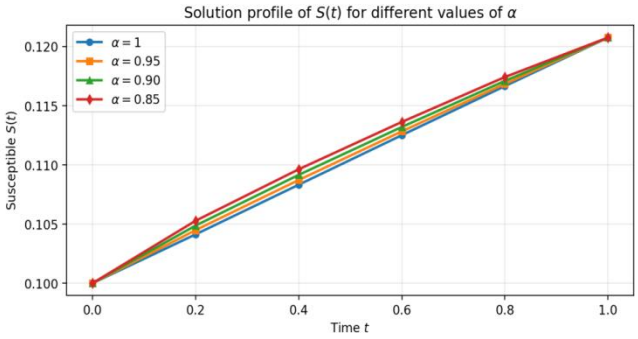

Fig. 1 Solution Profile of S (t) for different values of α

Observation from Figure 1 (Susceptible population S (t)): Figure 1 illustrates the temporal evolution of the susceptible population S(t) for different values of the fractional order α=1, 0.95, 0.90, and 0.85 .It is observed that the susceptible class increases gradually with time for all considered values of α. This growth is primarily due to the continuous recruitment of individuals into the susceptible class through births and the waning of vaccine-induced immunity.

A clear ordering of the solution curves is evident for smaller values of the fractional order α, the susceptible population attains slightly higher values at the same time instant. This behavior reflects the memory effect introduced by the fractional derivative. As α decrease, past states exert a stronger influence on the present dynamics, resulting in a slower depletion of susceptible individuals due to infection and a comparatively enhanced accumulation over time.

For α=1, corresponding to the classical integer-order model, the susceptible population exhibits the lowest trajectory among all cases, indicating a faster system response and weaker memory effects. In contrast, the fractional-order cases α <1 demonstrate smoother and more persistent dynamics, which are consistent with the hereditary nature of real epidemic processes.

Overall, Figure 1 confirms that the fractional-order model provides additional flexibility in capturing the temporal behavior of the susceptible population and highlights the significant role of memory effects in the transmission dynamics of Hepatitis B.

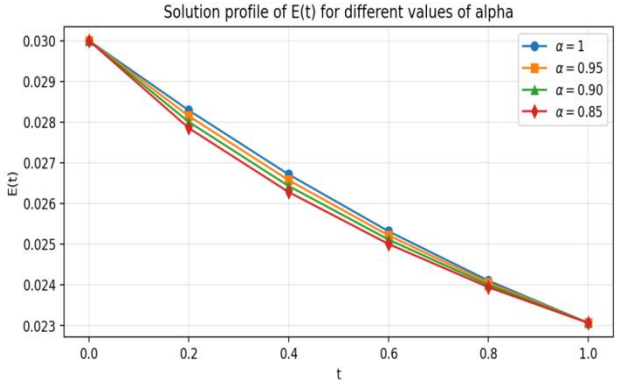

Fig. 2 Solution Profile of E(t) for different values of α

Observation from Figure 2 (Exposed population E(t)) Figure 2 depicts the temporal evolution of the exposed population E(t)) for different values of the fractional order α=1, 0.95, 0.90, and 0.85. It is clearly observed that the exposed class decreases monotonically with time for all considered values of α. This decline reflects the progression of exposed individuals into the acute infected class, as well as natural removal from the system.

A noticeable separation among the solution curves can be observed. For smaller values of the fractional order α, the exposed population remains slightly higher at the same time instant compared to the classical case. This behavior highlights the memory effect associated with fractional derivatives. As α decreases, the influence of past exposure states becomes stronger, leading to a slower transition from the exposed class to the infected class.

For α=1, corresponding to the integer-order model, the exposed population decays more rapidly, indicating a faster system response with negligible memory effects. In contrast, the fractional-order cases α<1 exhibit smoother and more gradual decay, which is more consistent with realistic incubation and latency processes in Hepatitis B infection.

Overall, Figure 2 demonstrates that the fractional-order formulation provides a more flexible and realistic description of exposed population dynamics by incorporating memory effects into the disease progression mechanism.

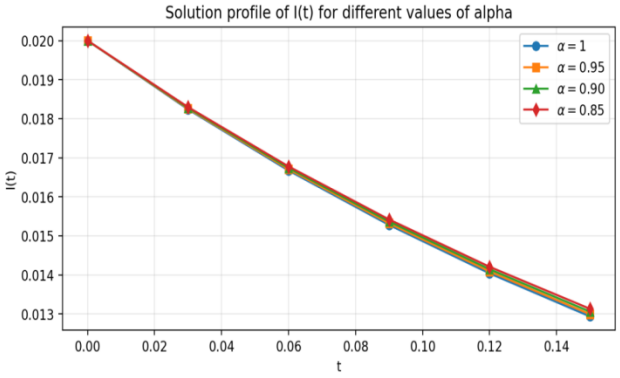

Fig.3 Solution profile of I(t) for different values of α

Observation from Figure 3 (Acute Infected Population I(t))

Figure 3 presents the temporal behavior of the acute infected population I(t) for different fractional orders α=1, 0.95, 0.90, and 0.85.It is observed that the number of acute infected individuals decreases with time for all considered values of α. This decline is mainly attributed to the progression of infected individuals either toward recovery or into the chronic carrier class, together with natural removal from the population.

A noticeable dependence on the fractional order is evident. For smaller values of α, the decay of the infected population is relatively slower, and the corresponding solution curves remain slightly above those of the classical case at the same time instant. This behavior reflects the memory effect inherent in the fractional-order model, where past infection states continue to influence the present dynamics.

In the classical case α =1, the infected population decreases more rapidly, indicating a faster system response with no memory effect. In contrast, for α <1, the fractional-order solutions exhibit smoother and

More persistent dynamics, which better represent the prolonged infectious period often observed in real Hepatitis B transmission processes.

Overall, Figure 3 highlights the significant role of fractional-order memory in modulating the decay rate of acute infections and demonstrates that the proposed fractional SEICRV model captures infection dynamics more realistically than its integer-order counterpart.

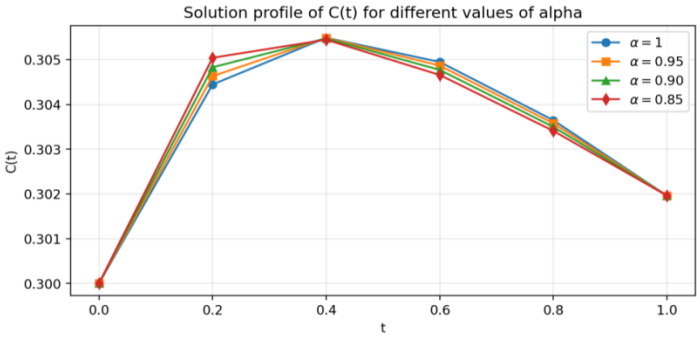

Fig.4 Solution profile of C (t) for different values of α

Observation from Figure 4 (Chronic carrier population C (t))

Figure 4 illustrates the temporal variation of the chronic carrier population C(t) for different values of the fractional order α=1,0.95, 0.90, and 0.85.It is observed that the carrier class exhibits a mild increase at early times, followed by a gradual decline as time progresses. This behavior reflects the inflow of individuals from the acute infected class and their subsequent removal due to recovery, treatment, and natural death. A clear influence of the fractional order is evident. For smaller values of α, the carrier population remains slightly higher at corresponding time instants, indicating a slower reduction of chronic carriers. This phenomenon arises from the memory effect introduced by the fractional derivative, which allows past infection states to persist and influence the current dynamics.

In the classical case α=1, the carrier population decreases more rapidly, demonstrating a quicker system response with no memory effect. In contrast, the fractional-order cases α<1 produce smoother and more prolonged carrier dynamics, which are consistent with the long-term persistence of chronic Hepatitis B infection observed in real populations.Overall, Figure 4 highlights the importance of fractional-order modeling in capturing the delayed clearance and persistence of chronic carriers and emphasizes the role of memory effects in shaping long-term disease dynamics.

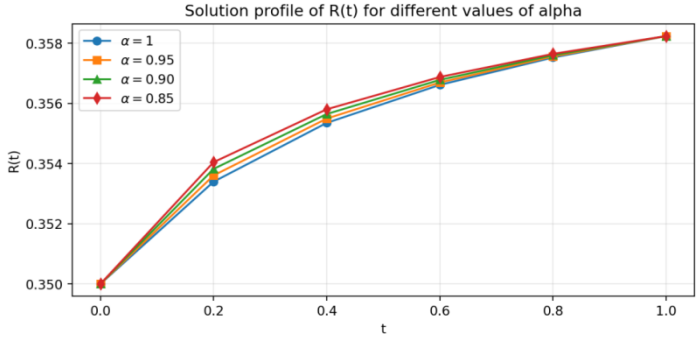

Fig.5 Solution profile of R (t) for different values of α

Figure 5 illustrates the temporal evolution of the recovered population R (t) for different values of the fractional order α=1, 0.95, 0.90, and 0.85. It is observed that the recovered class increases monotonically

with time for all considered values of α. This increasing trend is mainly due to recovery from both the acute infected and chronic carrier classes, as well as treatment-induced recovery.

A clear influence of the fractional order can be seen in the solution profiles. For smaller values of α, the recovered population attains slightly higher values at the same time instant. This behavior reflects the memory effect introduced by the fractional derivative, which enhances the cumulative impact of past infections and recoveries on the present state.

In the classical case α=1, the growth of the recovered population is comparatively slower, indicating a faster system response with weaker memory effects. In contrast, the fractional-order cases α<1 exhibit smoother and more persistent growth patterns, which are consistent with the gradual immune response observed in real Hepatitis B dynamics.

Overall, Figure 5 demonstrates that the fractional-order formulation provides a more realistic description of recovery dynamics and highlights the important role of memory effects in shaping the long-term behavior of the recovered population.

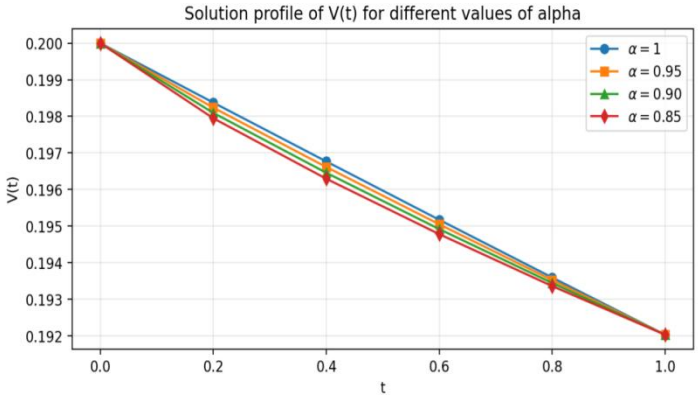

Fig.6 Solution profile of V (t) for different values of α

Figure 6 depicts the temporal evolution of the vaccinated population V(t) for different values of the fractional order α=1, 0.95, 0.90, and 0.85. It is observed that the vaccinated class decreases gradually with time for all considered values of α. This declining trend is primarily attributed to the waning of vaccine-induced immunity and natural removal from the population.

The influence of the fractional order is clearly visible. For smaller values of α, the vaccinated population remains slightly higher at corresponding time instants compared to the classical case. This behavior reflects the memory effect inherent in the fractional-order model, which allows past vaccination history to exert a prolonged influence on the current dynamics, thereby slowing the effective loss of vaccinated individuals.

In the classical case α = 1, the vaccinated population declines more rapidly, indicating a faster system response with no memory effect. In contrast, the fractional-order cases α < 1 exhibit smoother and more persistent decay patterns, which are consistent with realistic immunological processes in which vaccine protection wanes gradually over time.

Overall, Figure 6 highlights the importance of incorporating fractional-order memory effects to accurately describe vaccination dynamics and immunity waning in Hepatitis B transmission models.

8 Conclusion

In this work, a modified fractional-order SEICRV model for Hepatitis B virus dynamics has been proposed by incorporating an explicit vaccinated compartment, waning of vaccine-induced immunity, and a carrier-directed treatment/control mechanism. The model is formulated using Caputo fractional derivatives to account for memory effects inherent in epidemic processes.

The positivity and boundedness of solutions are rigorously established within a biologically feasible invariant region, ensuring the well-posedness of the model. The basic reproduction number is derived and shown to provide a clear threshold criterion for disease persistence or elimination. Furthermore, a detailed Laplace–Adomian Decomposition Method (LADM)is developed for the nonlinear fractional system, including explicit Adomian polynomials for the bilinear infection terms and a complete recursive solution scheme.

Numerical results for different fractional orders demonstrate the significant impact of memory effects on the transient dynamics of all compartments. The proposed fractional-order framework offers additional flexibility compared to classical integer-order models and provides a useful foundation for future studies involving parameter sensitivity analysis, optimal control strategies, and fitting to real epidemiological data**.**

References

1. I. Podlubny, Fractional Differential Equations*,* Academic Press, San Diego, 1999.
2. A. A. Kilbas, H. M. Srivastava and J. J. Trujillo, Theory and Applications of Fractional Differential Equations*,* Elsevier, Amsterdam, 2006.
3. K. Diethelm, The Analysis of Fractional Differential Equations, Springer, Berlin, 2010.
4. M. Caputo, Linear models of dissipation whose Q is almost frequency independent, Geophys. J. R. Astron. Soc.13 (1967), 529–539.
5. F. Mainardi, Fractional Calculus and Waves in Linear Viscoelasticity*,* Imperial College Press, London, 2010.
6. G. Adomian, Solving Frontier Problems of Physics: The Decomposition Method, Kluwer Academic Publishers, Dordrecht, 1994.
7. A. M. Wazwaz, Partial Differential Equations and Solitary Waves Theory, Springer, Berlin, 2009.
8. V. Daftardar-Gejji and H. Jafari, An iterative method for solving nonlinear functional equations, J. Math. Anal. Appl**.**316 (2006), 753–763.
9. Y. Luchko, Maximum principle for the generalized time-fractional diffusion equation, J. Math. Anal. Appl**.**351 (2009), 218–223.
10. W. O. Kermack and A. G. McKendrick, A contribution to the mathematical theory of epidemics, Proc. Roy. Soc. Lond. Ser. *A*115 (1927), 700–721.
11. Diekmann, O., Heesterbeek, J. A. P., and Britton, T., Mathematical Tools for Understanding Infectious Disease Dynamics*,* Princeton University Press, Princeton, 2010.
12. A. Atangana and J. F. Gómez-Aguilar, Numerical approximation of Riemann–Liouville and Caputo derivatives, Math. Model. Nat. Phenom.12 (2017), 1–17.
13. J. Singh, D. Kumar and D. Baleanu, On the analysis of fractional epidemiological models, Chaos Solitons Fractals140 (2020), 110073.
14. Hethcote, H. W., The mathematics of infectious diseases*,* SIAM Review,42(2000), 599–653.
15. C. Li and F. Zeng, Numerical Methods for Fractional Calculus*,* CRC Press, Boca Raton, 2017.